MADRID
inter.noise 2019
June 16 - 19
NOISE CONTROL FOR A BETTER ENVIRONMENT

Ocean-acoustic raytracing propagation models based on Fermat's least time principle

Raposo, Pedro[1]
CINAV (Navy Research Center)/EN (Naval Academy)
2810-001 Almada, Portugal

Gatta, Mário[2]
CINAV (Navy Research Center)/EN (Naval Academy)
2810-001 Almada, Portugal

Moreira, Miguel[3]
CINAV (Navy Research Center)/EN (Naval Academy)/CENTEC (Center of Marine Technology and Ocean Engineering)
2810-001 Almada, Portugal

ABSTRACT

Considering Fermat's least time principle we developed $2D$ and $3D$ ocean-acoustic raytracing propagation models. Each one consists of an algebraic differential system of equations. So, considering Fermat's least time principle we developed $2D$ and $3D$ ocean-acoustic parametric raytracing propagation models based on the Euler-Lagrange equations. Each one consists of an algebraic differential system of equations. Numerical simulations were presented, discussed and compared with propagation predictions obtained with a consolidated tool developed and utilized by the scientific community.

Keywords: Heterogeneous media, Raytracing, Ocean-acoustic propagation
I-INCE Classification of Subject Number: 76
(see http://i-ince.org/files/data/classification.pdf)

[1]amaral.raposo@marinha.pt
[2]mario.gatta@marinha.pt
[3]miguel.moreira@marinha.pt

1. INTRODUCTION

The study of underwater sound propagation is of prime importance. Indeed, in the underwater environment, contrary to electromagnetic waves which have small propagation ranges, acoustic waves can be used to communicate, detect objects and map the environment, among other uses [1]. It can be shown that sound wave propagation can be modeled as acoustic rays, namely above a well-defined sound frequency [2]. So, considering Fermat's least time principle we developed $2D$ and $3D$ ocean-acoustic parametric raytracing propagation models based on the Euler-Lagrange equations. Each one consists of an algebraic differential system of equations. Numerical simulations were presented, discussed and compared with propagation predictions obtained with a consolidated tool developed by Val Schimdt, [3] and used by the scientific community.

2. EULER-LAGRANGE'S EQUATIONS

Considering the parametrization $\mathbf{r}(\tau) = (x(\tau), y(\tau))$, $a \leq \tau \leq b$ of a $2D$ acoustic trajectory γ under a velocity sound field $v = v(x, y)$, Fermat's least time principle states that γ minimizes the trajectory time $t_{A\to B}$:

$$t_{A\to B} = \int_A^B \frac{ds}{v(x,y)} = \int_a^b \frac{\sqrt{\left(\frac{dx}{d\tau}\right)^2 + \left(\frac{dy}{d\tau}\right)^2}}{v(x,y)} d\tau. \tag{1}$$

It can be shown, see fot instace [4], that the integral of function F

$$F(\tau, x, y, x', y') = \frac{\sqrt{\left(\frac{dx}{d\tau}\right)^2 + \left(\frac{dy}{d\tau}\right)^2}}{v(x,y)}, \tag{2}$$

is minimized if F satisfies the Euler-Lagrange's equations:

$$\begin{cases} \frac{d}{d\tau}\left(\frac{\partial F}{\partial x'}\right) - \frac{\partial F}{\partial x} = 0 \\ \frac{d}{d\tau}\left(\frac{\partial F}{\partial y'}\right) - \frac{\partial F}{\partial y} = 0 \end{cases}. \tag{3}$$

Thus, deducing,

$$\frac{\partial F}{\partial x} = -\frac{\partial v}{\partial x}\frac{\sqrt{(x')^2 + (y')^2}}{v^2}, \tag{4}$$

$$\frac{\partial F}{\partial x'} = \frac{x'}{v\sqrt{(x')^2 + (y')^2}}, \tag{5}$$

$$\frac{d}{d\tau}\left(\frac{\partial F}{\partial x'}\right) = -\frac{\left((x')^4 + (y')^2(x')^2\right)\frac{\partial v}{\partial x} + \left(x'y'y'' - (x')^2(y')^2\right)v + \left((x')^3 y' + (y')^3 x'\right)\frac{\partial v}{\partial y}}{v^2\sqrt{\left((x')^2 + (y')^2\right)^3}}. \tag{6}$$

and calculating also $\frac{\partial F}{\partial y}$, $\frac{\partial F}{\partial y'}$e $\frac{d}{d\tau}\left(\frac{\partial F}{\partial y'}\right)$ one can establish from (3) the corresponding Euler-Lagrange's equations:

$$\begin{cases} x''y' - y''x' + \frac{1}{v}\frac{\partial v}{\partial x}\left((y')^3 + (x')^2 y'\right) - \frac{1}{v}\frac{\partial v}{\partial y}\left((x')^3 + (y')^2 x'\right) = 0 \\ y''x' - x''y' + \frac{1}{v}\frac{\partial v}{\partial y}\left((x')^3 + (y')^2 x'\right) - \frac{1}{v}\frac{\partial v}{\partial x}\left((y')^3 + (x')^2 y'\right) = 0 \end{cases}. \tag{7}$$

The solution $\mathbf{r}(\tau) = (x(\tau), y(\tau))$, $\tau \in [a, b]$ of this system of second order differential equations will correspond to the desired $2D$ acoustic trajectory, that minimizes (1). Unfortunately, these equations are singular because they are symmetric.

Assuming now a $3D$ ray trajectory parametrized by $\mathbf{r}(\tau) = (x(\tau), y(\tau), z(\tau))$, $a \leq \tau \leq b$ and using an identical approach one can establish the $3D$ Euler-Lagrange's equations which minimize the acoustic trajectory time $t_{A\to B}$ given by:

$$t_{A\to B} = \int_A^B \frac{ds}{v(x,y,z)} = \int_a^b \frac{\sqrt{\left(\frac{dx}{d\tau}\right)^2 + \left(\frac{dy}{d\tau}\right)^2 + \left(\frac{dz}{d\tau}\right)^2}}{v(x,y,z)} d\tau. \tag{8}$$

After some algebraic work one obtain:

$$\begin{cases} \left((y')^2 + (z')^2\right) x'' v - \left(y'y'' + zz''\right) x' v - \left((x')^2 + (y')^2 + (z')^2\right) x' \frac{dv}{d\tau} \\ \qquad + \frac{\partial v}{\partial x}\left((x')^2 + (y')^2 + (z')^2\right)^2 = 0 \\ \left((x')^2 + (z')^2\right) y'' v - \left(x'x'' + z'z''\right) y' v - \left((x')^2 + (y')^2 + (z')^2\right) y' \frac{dv}{d\tau} \\ \qquad + \frac{\partial v}{\partial y}\left((x')^2 + (y')^2 + (z')^2\right)^2 = 0 \\ \left((y')^2 + (x')^2\right) z'' v - \left(y'y'' + x'x''\right) z' v - \left((x')^2 + (y')^2 + (z')^2\right) z' \frac{dv}{d\tau} \\ \qquad + \frac{\partial v}{\partial z}\left((x')^2 + (y')^2 + (z')^2\right)^2 = 0 \end{cases}. \tag{9}$$

Unfortunately, these equations are also singular because system (9) is of rank two.

In upcoming sections we will describe the approach used to obtain the $2D$ and $3D$ models for the acoustic ray propagation overcoming the problem point out.

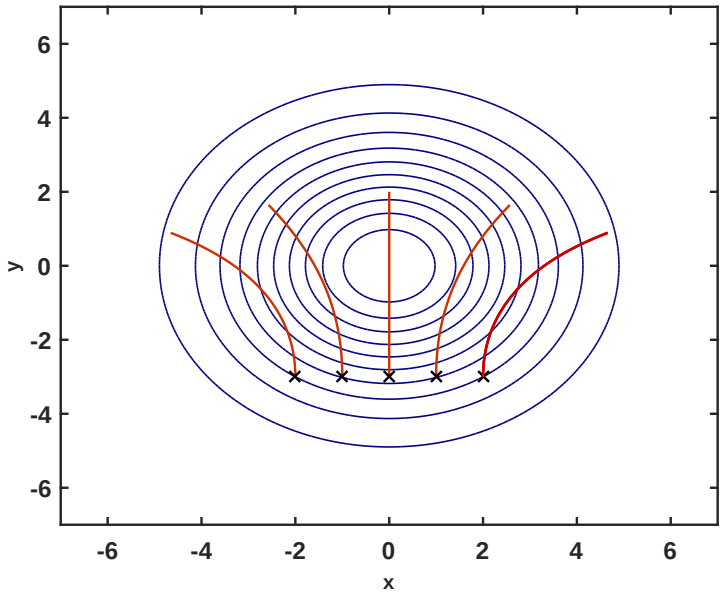

Figure 1: Some rays lauched from the line $y = -3$ and with an initially y-orientation.

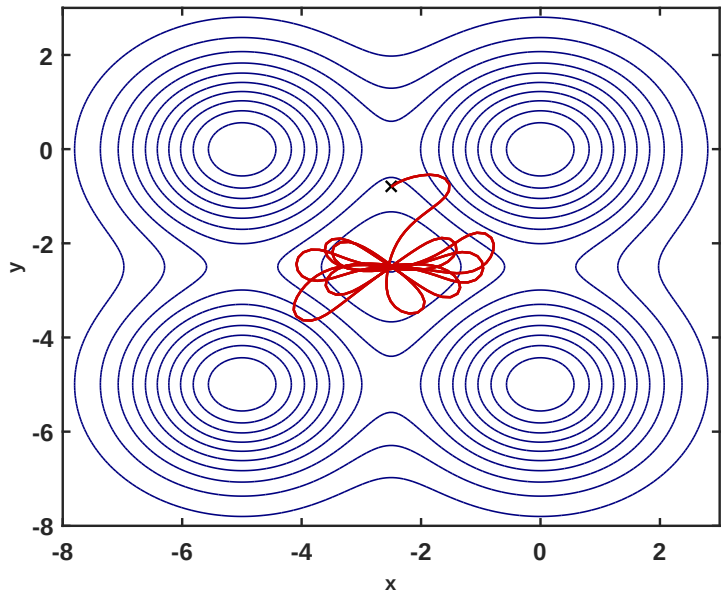

Figure 2: An arbitrary ray traveling through a complex and virtual sound field.

3. ESTABLISHMENT OF THE 2D MODEL

In order to close the $2D$ problem (7) we must replace one of the deduced equations by a mathematically and physically relevant equation. Note that

$$t_{A\to B} = \int_a^b \frac{\sqrt{(x')^2 + (y')^2}}{v(x,y)} d\tau = \int_\gamma \frac{ds}{v(x,y)}, \tag{10}$$

does not depend on the choosen parametrization $\mathbf{r}(\tau) = (x(\tau), y(\tau))$, $a \leq \tau \leq b$, as long as $\mathbf{r} = \mathbf{r}(\tau)$ fulfills natural conditions of regularity such as being of class C^1 and satisfying $\mathbf{r}'(\tau) \neq \mathbf{0}$, $\forall \tau \in]a, b[$, see for instance [5]. In other words, the information needed to solve this system, which will be written in the form of a new equation, is simply the selection of a parametrization among a group of possible ones. So, to close the problem we can simply adopt the condition

$$\|\mathbf{r}'(\tau)\|^2 = 1, \tag{11}$$

which is equivalent to consider the arc legth $s(\tau) = \int_a^\tau \|\mathbf{r}'(t)\| dt$ parametrization of $\mathbf{r}(s) = (x(s), y(s))$ because

$$\left\| \frac{d\mathbf{r}}{ds} \right\| = 1. \tag{12}$$

Bearing in mind equation (11) we can infer the following simplifications on (7) and obtain:

$$\begin{cases} x' - z = 0 \\ y' - w = 0 \\ z'w - w'z + \frac{w}{v}\frac{\partial v}{\partial x} - \frac{z}{v}\frac{\partial v}{\partial y} = 0 \\ z^2 + w^2 - 1 = 0 \end{cases}. \tag{13}$$

The established $2D$ model (13) is a system of differential algebraic equations (see for instance [6]) which have to be numericaly solved using an implicit algorithm.

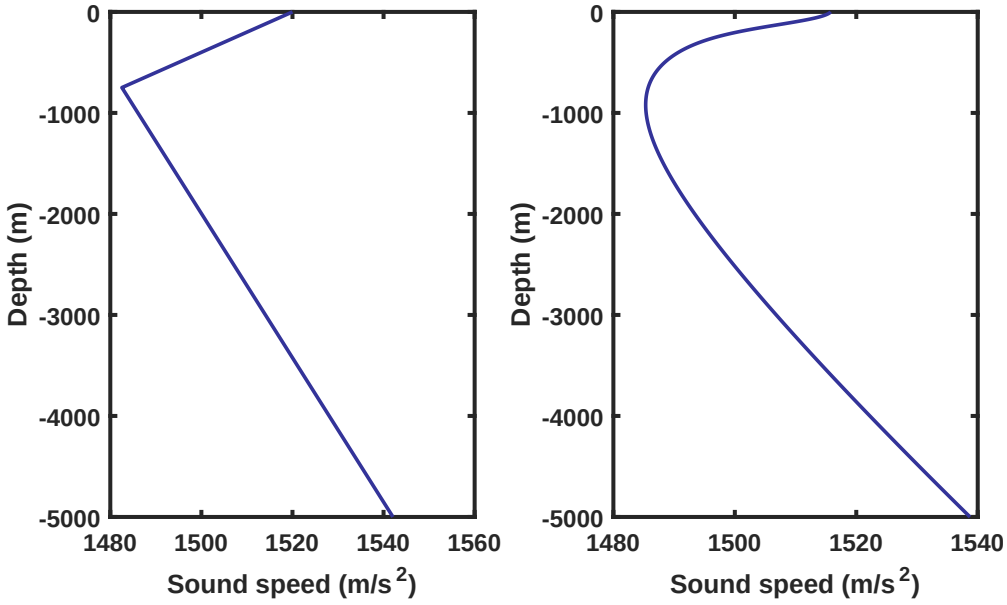

Figure 3: Sound speed profiles used to compare the models.

We found advantage in changing the stiff purely algebraic last equation of (13)

$$z^2 + w^2 = 1,$$

by the softer one

$$zz' + ww' = 0. \tag{14}$$

Note that (14) implies the invariance of the trajectory tangent vector's norm. So, (11) and (14) are equivalente whenever for some τ, $\|\mathbf{r}'(\tau)\|^2 = 1$ and this happens if we define initial conditions according. Thus, the adopted final $2D$ model is written as:

$$\begin{cases} x' - z = 0 \\ y' - w = 0 \\ z'w - w'z + \frac{w}{v(x,y)}\frac{\partial v}{\partial x} - \frac{z}{v(x,y)}\frac{\partial v}{\partial y} = 0 \\ zz' + ww' = 0 \end{cases}. \tag{15}$$

To numerically solve (15) we used a robust algorithm, developed in MATLAB by Tony Roberts [7], suitable for differential algebraic systems.

4. 2D NUMERICAL SIMULATIONS

4.4.1. Preliminary numerical simulations

In order to preliminary test model (15) we defined Gaussian sound velocity fields, such as

$$v(x,y) = k_1 e^{-k_2((x-x_0)^2+(y-y_0)^2)} \text{ and} \tag{16}$$

$$v(x,y) = k_1\left(1 - e^{-k_2((x-x_0)^2+(y-y_0)^2)}\right), \tag{17}$$

with $k_1 > 0$ and $k_2 > 0$. Note that, at position (x_0, y_0) the velocity field (16) attains its maximum value while (17) attains its the minimum value.

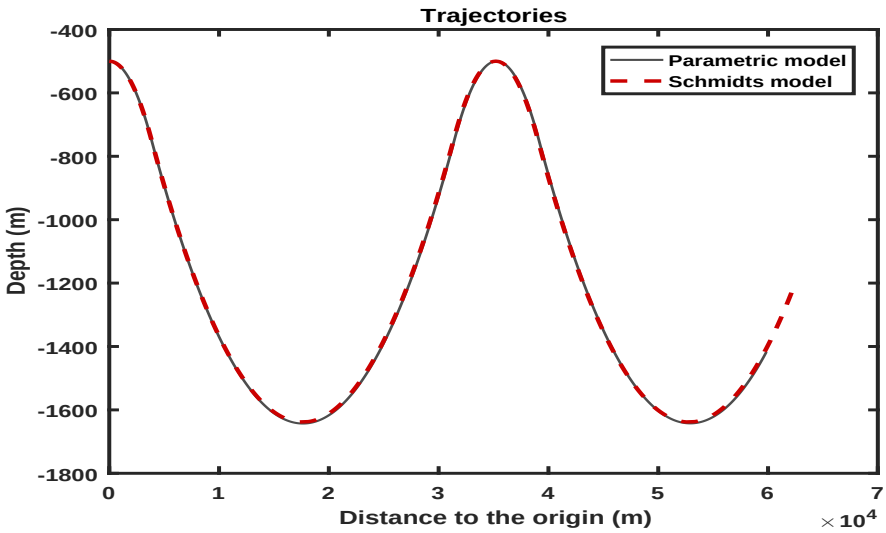

Figure 4: Comparison between Schimdt's tool and our parametric model using a linear sound velocity profile.

In Figure 1 some initially $y-$oriented trajectories in a region with a velocity field of type (16) are illustrated. With the exception of the acoustic ray starting at position $(0,-3)$, the rays bend in the direction of lower sound velocity as we expected according to Snell's law. The acoustic ray starting at position $(0,-3)$ maintains a rectilinear trajectory compatible with the symmetry associated with the configuration of the trajectory.

In Figure 2 the $2D$ model (15) is tested in a region with a complex sound velocity field consisting of a linear combination of (16) and (17) type sound velocity fields with extrema in different locations. We can observe that the model can generate the expected complex trajectories apparently without the Snell's law being violated.

4.4.2. Comparision with raytracing software

To be able to predict ocean-acoustic ray propagation in vertical planes Val Schimdt [3] developed a $2D$ raytracing tool which has been extensively used by the scientific community. In this section we are going to compare raytrace Val Schimdt's predictions with those obtained from our $2D$ (15) model. Note that in Schimdt's tool the sound speed variations are approximated by piecewise linear gradients. Under this assumption, sound travels through each layer as a circular arc.

Differently from Schmidt's tool, that uses a discrete data set for the sound speed profile, our $2D$ model needs a class C^1 function (except for a finite number of points) describing the sound field. So, we assumed a constant water salinity of 35 ppm and we adopted the following water temperature profile established by Joseph [8], where T_s is the surface's water temperature:

$$T(y) = -0.338 + \frac{(T_s + 0.338)\left(1 + e^{-0.016y+1.244}\right)}{(1.485 \times 10^{-4})(T_s + 0.338)\, y + (1 + e^{-0.016y+1.244})}. \tag{18}$$

The sound speed profile given the temperature T (in Celsius degrees), the depth D (in meters) and the salinity S (in parts per million) was analyticaly computed using

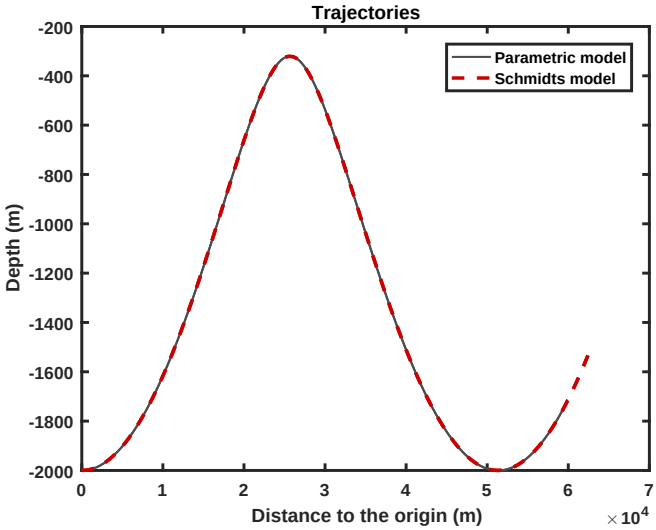

Figure 5: Comparison between Schimdt's tool and our parametric model using a realistic sound velocity profile.

Makenzie's sound velocity equation [9] and (18)

$$c(D,S,T) = \tag{19}$$
$$= a_1 + a_2T - a_3T^2 + a_4T^3 + a_5S^* + a_6D + a_7D^2 - a_8TS^* - a_9TD^3,$$

where

$$\begin{aligned} S^* &= S - 35 \text{ and} \\ a_1 &= 1448.96 \\ a_2 &= 4.591 \\ a_3 &= -5.304 \times 10^{-2} \\ a_4 &= 2.374 \times 10^{-4} \\ a_5 &= 1.340 \\ a_6 &= 1,630 \times 10^{-2} \\ a_7 &= 1,675 \times 10^{-7} \\ a_8 &= -1,025 \times 10^{-2} \\ a_9 &= -7,139 \times 10^{-13} \end{aligned}$$

In Figure 3 we ilustrate the two sound profiles used in the numerical simulations performed here. In the left sound speed profile the velocity gradient is constant. The more realistic right sound profile was computed using (19).

In Figure 4 one can observe raytrace predictions from Schmidt's tool and our $2D$ parametric model using the linear picewise sound velocity profile (the left sound velocity profile of Figure 3). Observe that in this situation Schmidt's tool provides accurate predictions since we are using a linear picewise sound velocity profile. We can verify that the predictions offered by our $2D$ parametric model and Schmidt's tool agree. This fact shows that the performance of our model, in this situation, is as rigorous as Schmidt's tool.

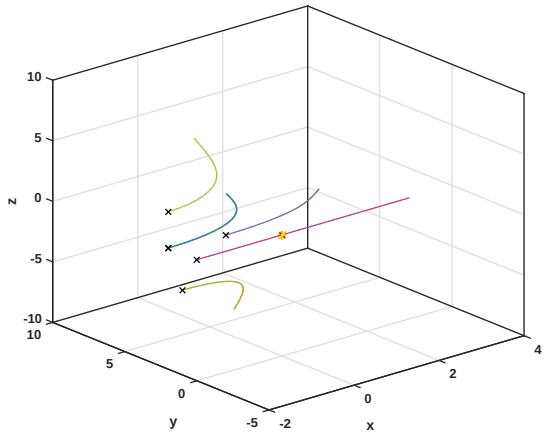

Figure 6: First view of the 3*D test: Some rays launched from arbitrary positions on the plane* $x = -2$ *and with an* $x-$*orientation through a sound field with a maximum velocity at* $(0, 0, 0)$*, represented by a yellow and red asterisk (*).*

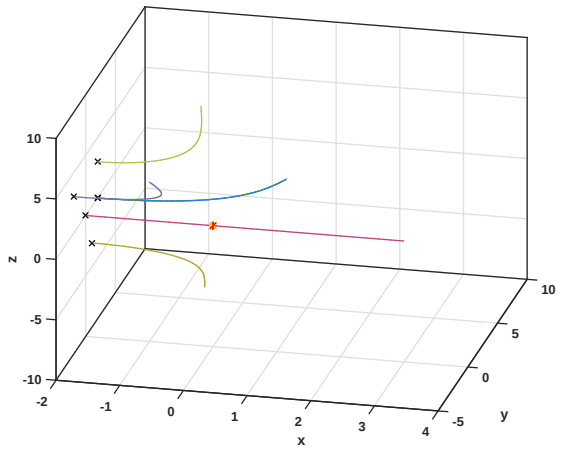

Figure 7: Second view of the 3*D test.*

In Figure 5 one can observe raytrace predictions between Schmidt's tool and our $2D$ parametric model using a more rigorous sound velocity profile (the right sound velocity profile of Figure 3). Both simulations agree demonstrating an adequate performance of our $2D$ parametric model.

5. ESTABLISHMENT OF THE 3D MODEL

As it was mentioned before the previously deduced $3D$ Euler-Lagrange's equations (9) are singular being of rank two.

Before we follow the approach used in the development of the $2D$ model we must preserve all the information of the three equations (9). This requirement is met by adding member-to-member the last equation to the first equation as well as to the second equation. We then replace the redundant last equation of the newly modified system (9) by the condition

$$x'x'' + y'y'' + z'z'' = 0,$$

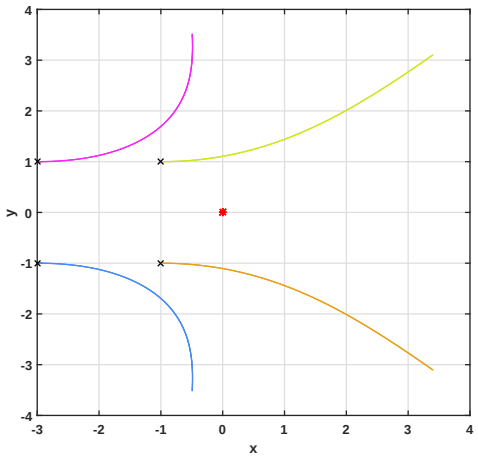

Figure 8: Trajectory prediction of some x−oriented launched (at $z = 0$ plane) acoustic rays.

which is equivalent to

$$\|\mathbf{r}'(\tau)\|^2 = 1,$$

if we define initial conditions according.

After some algebraic work and first order reduction we obtain finally our $3D$ parametric model:

$$\begin{cases} x' - a = 0 \\ y' - b = 0 \\ z' - c = 0 \\ \left(1-a^2\right)a' + \left(1-c^2\right)c' - ac\,(a'+c') - b\,(ab'+cb') \\ \quad + \frac{1}{v}\left(\frac{\partial v}{\partial x} + \frac{\partial v}{\partial z} - \left(\frac{dv}{dx}a + \frac{dv}{dy}b + \frac{dv}{dz}c\right)(a+c)\right) = 0 \\ \left(1-b^2\right)b' + \left(1-c^2\right)c' - bc\,(b'+c') - a\,(ba'+ca') \\ \quad + \frac{1}{v}\left(\frac{\partial v}{\partial y} + \frac{\partial v}{\partial z} - \left(\frac{dv}{dx}a + \frac{dv}{dy}b + \frac{dv}{dz}c\right)(b+c)\right) = 0 \\ aa' + bb' + cc' = 0 \end{cases}. \tag{20}$$

Some numerical simulations using the robust algorithm developed in MATLAB by Tony Roberts [7] will be presented in the next section.

6. 3D NUMERICAL SIMULATIONS

In order to preliminary test our $3D$ model (20), and considerering $k_1 > 0$ as well as $k_2 > 0$, the following $3D$ Gaussian type velocity model were defined:

$$v(x,y,z) = k_1 e^{-k_2((x-x_0)^2+(y-y_0)^2+(z-z_0)^2)}. \tag{21}$$

In Figures 6 and 7 we display the predicted trajectories of some rays $x-$oriented launched from arbitrary at plane $x = -2$ in a region with a velocity field of type (21). With the exception of the acoustic ray starting at position $(-2, 0, 0)$, the rays bend in the direction of lower sound velocity as we expected according to Snell's law. The acoustic ray starting at position $(-2, 0, 0)$ maintains a rectilinear trajectory compatible with the symmetry associated with the configuration of the trajectory.

In Figure 8 we display the predicted trajectories of some rays $x-$oriented launched from positions $(-3,1,0)$, $(-3,-1,0)$, $(-1,-1,0)$ and $(-1,-1,0)$, in a region with the same velocity type field. One can observe that the predicted ray trajectories remain in the same plane as is expected.

The results of the numerical simulations performed here seem to be satisfactory. However it will be necessary to carry out later in an upcoming work an adequate validation of the results of our $3D$ acoustic ray propagation model.

7. CONCLUSIONS

Taking into account the simulations and the arguments presented, we can draw the following conclusions:

- The trajectories generated by our $2D$ model (15) seems to be sufficiently robust to accommodate the simulation of complex trajectories.
- The trajectories generated by our $2D$ model and by Schimdt's raytracing tool coincide in regions corresponding to common domains of use.
- Despite the need for adequate future validation of our $3D$ model (20) preliminary numerical simulations suggest that it perform satisfactory.

8. FUTURE WORK

Based on the $2D$ (15) and $3D$ (20) parametric models of sound propagation presented we envisage the following upcoming developments:

- Perform an appropriate validation of the $3D$ model.
- Develop the possibility of simulation $2D$ and $3D$ acoustic ray trajectories the presence of reflections.

9. ACKNOWLEDGEMENTS

We acknowledge CINAV the Portuguese Navy's Research Centre and the Portuguese Naval Academy (EN) for the support and funding which was essential to the development and presentation of this work.

10. REFERENCES

[1] Paul C. Etter. Advanced applications for underwater acoustic modeling. *Advances in Acoustics and Vibration*, 2012, 2012.

[2] Michael J. Buckingham. Ocean-acoustic propagation models. *J. Acoustique*, pages 223–287, jun 1992.

[3] Val Schmidt. Raytrace. MATLAB, 2009.

[4] Cornelius Lanczos. *The Variational Principles of Mechanics*. Uni. Toronto Press, 1952.

[5] Tom Apostol. *Calculus, Vol. 2*. Reverté, 1993.

[6] U. M. Ascher and L. R. Petzold. *Computer Methods for Ordinary Differential Equations and Differential Algebraic Equations*. SIAM, 1998.

[7] Tony Roberts. Differential algebraic equations solver dae. Technical report, University of Southern Queensland, 1998.

[8] Joseph. The temperature of ocean water at a given depth, 2010.

[9] NPL. Technical guides - speed of sound in sea-water, 2000.